JOURNAL OF MATERIALS SCIENCE 28 (1993) 5637–5647

The long-term corrosion of glass by groundwater

G. A. COX, B. A. FORD
Department of Physics, University of York, York YO1 5DD, UK

Specimens of corroded soda and potash glasses, which had been exposed to groundwater for periods of up to about 1650 years, have been physically and chemically analysed. The morphology and compositional profiles of their finely laminated weathering crusts were determined by scanning electron microscopy and electron-probe microanalysis. It is shown that the surface layers on all specimens are depleted, to varying extents, of their principal constituents, with the exception of Si, Al and Fe. X-ray and electron diffraction studies have revealed the (tentative) identities of complex, poorly crystalline silicates and aluminosilicates within the largely amorphous crusts on potash glasses. The mean thickness of the crusts was found to correlate well with the free energy of hydration, ΔG°, of the pristine glasses. The rate of layer formation on the most durable specimens ($\Delta G^\circ \approx -15$ kJ mol^{-1}) was about 4×10^{-3} μm year^{-1}. Deposits of calcite, calcium phosphate and manganese rich minerals occurred within the crusts; they were largely of external origin. Thus, in addition to the composition of the glass, the geochemistry of the local groundwater plays a decisive role in determining the identity of the compounds present within the weathering crusts.

1. Introduction

The corrosion of glass by aqueous media has attracted world-wide attention in recent years. The stimulus has been the decision, taken by several countries, to immobilize high-level nuclear waste by vitrifying it, followed by long-term storage (10^3–10^5 years) in deep, geologically stable repositories. Eventually, the engineered and natural barriers which isolated this hazardous product from its environment will fail, allowing groundwater to come into contact with the vitrified waste. Ion exchange (leaching), possibly accompanied by more aggressive aqueous attack (matrix dissolution), will cause the glass to decay, with the consequent release of radioactive species into the biosphere. The safe disposal of high-level waste (HLW) evidently calls for a clear understanding of the factors which govern the aqueous corrosion of glass.

There is an extensive literature on the short-term, accelerated corrosion of silicate glasses (mainly candidate HLW glasses) under hydrothermal conditions [1]. Data from experiments carried out over days or months are used to predict the long-term behaviour of specimens under conditions more typical of those which will prevail in a repository. Destructive changes are modelled and the modifying influence of secondary, precipitated phases are examined [2].

In contrast, the natural degradation of glass by groundwater has received far less attention. This is, however, an important aspect of glass corrosion studies for the following reasons. First, the performance of specimens which have already undergone long-term weathering (centuries to millennia) is already known. Second, the geochemical reactions which occur at ambient temperatures between glass and groundwater—a complex medium containing ions in solution and suspended matter—may lead to different end products *vis-à-vis* those formed at elevated temperatures in laboratory tests. Depending upon the composition of the specimens, data from such studies have a relevance to problems as diverse as the disposal of HLW and the conservation of excavated vitreous artefacts.

Possibly the earliest detailed description of naturally decomposed glass was published by Brewster [3] in 1863, who commented upon its iridescent, flaky surface. Archaeologists have long been aware that glass recovered from damp soil often has a laminated weathering crust. Morphological studies of such crusts were reported by Raw [4] and Geilmann [5] during the 1950s. They found that when viewed in cross-section, the crusts were composed of fine, regularly spaced layers whose separation was typically within the range 5–20 μm. Bulk chemical analyses showed that the corrosion products contained little of the alkali present in the original glass and that heavy metals had entered from the environment [5]. Brill and Hood [6] suggested that there was a direct relation between the number of layers of corrosion present on the surface of a given specimen and the number of years it had remained buried, one layer being deposited per annum. Annual excursions in soil temperature and water content were believed to be the cause of this periodic process. However, evidence has accumulated to show that such a simple interpretation is improbable [7]. Indeed, surface layers are commonly formed on glass when it is subjected to constant temperature

0022–2461

leaching experiments in the laboratory—see, for example, Malow [8].

In this paper we report analytical and morphological studies of the weathering products on alkali–lime–silica glasses that have been exposed to groundwater for periods of up to approximately 1650 years. In a previous paper [9], the present authors discussed the natural corrosion of glass under marine conditions.

2. Experimental procedure

The corroded glasses were of archaeological origin; they were obtained from five sites in England. All were fragments of window glass, brief details of which are given in Table I, together with pH values of the soils from which they were recovered. Specimens from Rievaulx had been exposed to fallen rubble and lime mortar [10]; the environment could therefore be expected to have a pH > 7. The unaltered glass was pale green (caused by the presence of iron as an impurity) with the exception of that from St. Augustine's Abbey, Canterbury, which varied from mid to dark green in colour.

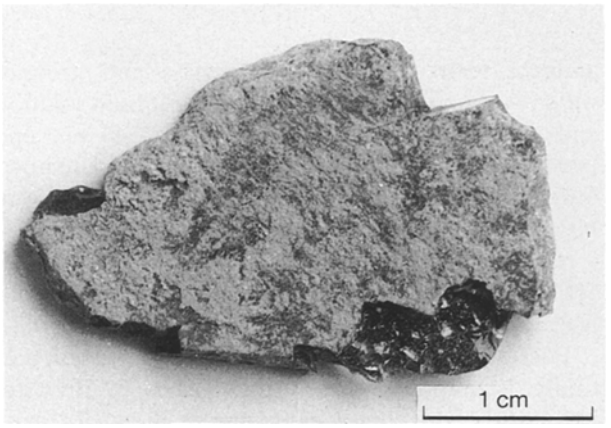

Figure 1 Specimen RA6 in the as-received state showing the weathering crust and the pristine glass.

Glass which has remained in contact with soil and groundwater for long periods of time commonly shows signs of decay. The durable specimens from Wroxeter had only a slight surface iridescence, whereas the less durable ones from the other sites had thick, opaque corrosion crusts which totally obscured the unaltered glass, as may be seen in Fig. 1. Depending upon the composition of the glass and local environmental conditions, crusts several millimetres in thickness were quite common. In extreme cases no traces of the original glass remained. On account of their laminated structure all corrosion crusts were fragile and ready exfoliated. The specimens selected for study retained their original surfaces; this was especially important for the determination of concentration profiles of the constituents of the crusts.

Selected pieces of corroded glass were vacuum impregnated with a 5% solution of Acryloid B-72 (Rohm & Haas Co) in acetone to consolidate the crusts. They were then sectioned and embedded in Epoxide resin (Buehler) followed by polishing with diamond paste to a 0.25 μm finish.

The polished sections were examined at low magnification with an optical microscope to establish the coarse structure of the crusts. Subsequently they were coated with carbon prior to a detailed examination in the scanning electron microscope (SEM). A Cambridge Instruments model 90B was used equipped with a Si(Li) X-ray detector (resolution 150 eV at 5.9 keV) and a Link Systems AN10000 X-ray analyser to permit electron-probe microanalysis (EPMA) to be carried out. Quantitative chemical analyses were obtained by subjecting net X-ray intensities to a ZAF correction programme [11]. The spatial resolution for quantitative analyses was approximately 5 μm. The operating conditions for EPMA were 15 kV acceleration voltage, 0.5 nA beam current.

The crust material was examined by electron and X-ray diffraction. The former was carried out using a Hitachi HU-11E transmission electron microscope (TEM). X-ray diffraction (XRD) patterns were obtained from powdered samples using a Phillips PW 1024/30 camera and filtered CuK_α radiation.

TABLE I Details of the specimens

Excavation site	Identifying prefix	Description of corrosion	Approximate date of burial (AD)[a]	pH of soil
Eltham Palace, Kent	EP	Dark-coloured corrosion crusts 0.5 to 1 mm in thickness	Before 1650	7.2
Rievaulx Abbey, N. Yorkshire	RA	Fragile corrosion crusts of irregular thickness. Localized coloured regions: red, brown, blue	*c.* 1540	Not known but > 7.0
Stamford Castle, Lincolnshire	SC	Dark-coloured corrosion crusts, some > 1 mm in thickness	*c.* 1200	7.6
St. Augustine's Abbey, Canterbury	SAA	Irregularly corroded specimens	Uncertain, probably *c.* 1540	7.8
Wroxeter, Shropshire	WRX	Very thin (< 40 μm) uniform corrosion, almost colourless	*c.*350	7.9

[a]Estimated, based upon archaeological context.

TABLE II Composition of the pristine glass

Specimen	Wt% of oxide													
	Na_2O	MgO	Al_2O_3	SiO_2	P_2O_5	K_2O	CaO	MnO	Fe_2O_3	CuO	PbO	S	Cl	Total
EP1	2.4	7.3	0.9	59.5	3.0	11.6	13.6	1.2	0.8					100.3
EP4	1.5	3.4	3.9	52.1	4.2	7.3	24.0	2.1	0.4					98.9
RA1	2.8	6.2	1.2	47.8	5.9	15.9	15.3	1.2	0.9				0.5	97.7
RA4	2.8	6.4	1.2	48.2	6.3	16.0	16.0	1.6	0.9					99.4
RA6	2.4	8.3	1.0	48.2	7.7	17.0	13.6	1.5	0.6					100.3
RA8	2.8	6.5	1.2	48.4	6.5	17.1	15.9	1.2	0.6				0.4	100.6
SC6	1.3	7.0	1.2	46.2	6.9	16.3	19.3	1.3	0.6					100.1
SC10	1.7	6.5	1.3	47.2	6.4	16.3	18.5	1.1	0.6					99.6
SC11	1.3	6.9	1.2	45.8	6.9	17.6	18.4	1.3	0.6					100.0
SAA1	2.7	6.5	1.2	55.7	3.1	11.0	13.1	1.0	0.6	2.3				97.2
SAA3	1.7	5.7	0.8	52.1	4.5	18.9	15.2	0.7	0.5					100.1
WRX1	17.4	0.6	1.9	70.8	0.1	0.9	6.3	0.5	0.5			0.3	0.8	100.1
WRX2	16.5	0.7	2.0	67.5	0.3	0.8	6.2	0.4	1.4	1.2	2.2		0.9	100.1
WRX6	15.4	0.6	2.4	72.1	0.1	0.4	7.4	< 0.1	0.4			0.1	1.2	100.1
WRX9	18.7	0.6	1.7	69.9	0.1	0.6	6.1	0.2	0.6	0.2		0.4	1.1	100.2
WRX10	17.4	0.5	1.7	70.5	0.1	0.7	6.1	0.5	1.1	0.2		0.2	1.1	100.1

Where no value is given that component was not detected.

Laser Raman microspectroscopy was also used to examine the crust material. The instrument (constructed at the University of York) was aligned so that a beam of radiation, approximately 1 μm in diameter from a 10 mW argon ion laser ($\lambda = 488$ nm) was incident on selected features within the crusts. Multiple scans of the same region could be carried out to enhance weak features.

3. Results

3.1. Composition of the pristine glasses

The specimens fell into two, well-defined groups according to the identity of the principal alkali present, their relative silica contents and the overall levels of alkaline earth oxides—see Table II. The influence of composition on the durability of glass is well exemplified by these results.

The largest group, comprised of material from Eltham Palace (EP), Rievaulx Abbey (RA), Stamford Castle (SC) and St Augustine's Abbey (SAA), were poorly durable potash glasses, as revealed by their thick weathering crusts. The second contained glasses from Wroxeter (WRX); their compositions were typical of durable soda glasses melted throughout the Roman provinces of Europe [12].

The potash glasses formed a relatively coherent group with compositions consistent with glasses melted in Western Europe between about the 11th and 15th centuries AD [13]. They are characterized by high K_2O contents (7.3–18.9 wt %), low Na_2O (1.3–2.8 wt %) and SiO_2 (45.8–59.5 wt %), but moderate amounts of MgO (3.4–8.3 wt %) and CaO (13.1–24.0 wt %). All of them contained appreciable quantities of P_2O_5 (3.0–7.7 wt %), indicative of wood ash, or that from terrestrial plants (as opposed to marine vegetation), being the chief source of alkali.

The specimens from Wroxeter had a markedly different composition. All had high Na_2O (15.4–18.7 wt %) and SiO_2 (67.5–72.1 wt %) contents. Other principal oxides were present at relatively moderate to low levels, for example CaO (6.1–7.4 wt %) and Al_2O_3 (1.7–2.4 wt %).

In both types of glass, iron and manganese were present at approximately the same concentrations, expressed in Table II in terms of Fe_2O_3 and MnO, respectively. Iron in the Fe(II) state colours glass an undesirable pale green; the presence of manganese may indicate a deliberate attempt to decolourize it by oxidizing the iron to the Fe(III) state.

3.2. Morphology of the weathering crusts

When viewed at low magnification in reflected light, the crusts on sectioned potash glasses showed wide variability of colour and structure. Opalescent, white bands extending over several millimetres were common, as were areas coloured yellow, red and brown — see Table I. Dark surface regions where material from the environment had intruded into the crusts were readily visible, as shown in Fig. 2, and were present in all of the potash glasses. The thin, translucent, greyish-white crusts on soda glasses did not show the same variability of colour; in reflected light they were iridescent.

A prominent feature of all the crusts was their finely laminated structure, as noted by previous investigators [3–7, 9]. Optical and scanning electron microscopy of sectioned specimens revealed wide variations of morphology. Each crust had unique features, depending primarily upon the composition of the original glass, its degree of homogeneity and the environment to which it had been exposed. The following morphological types were distinguished.

1. Parallel layers (Fig. 3a). Consecutive lamellae were almost parallel to each other and to the surface of the original glass, from where the corrosion front (reaction zone) had progressed in a regular, undisturbed manner into the body of the specimen. This structure occurred locally in all of the crusts, irrespective of the composition of the pristine glass. Inter-layer

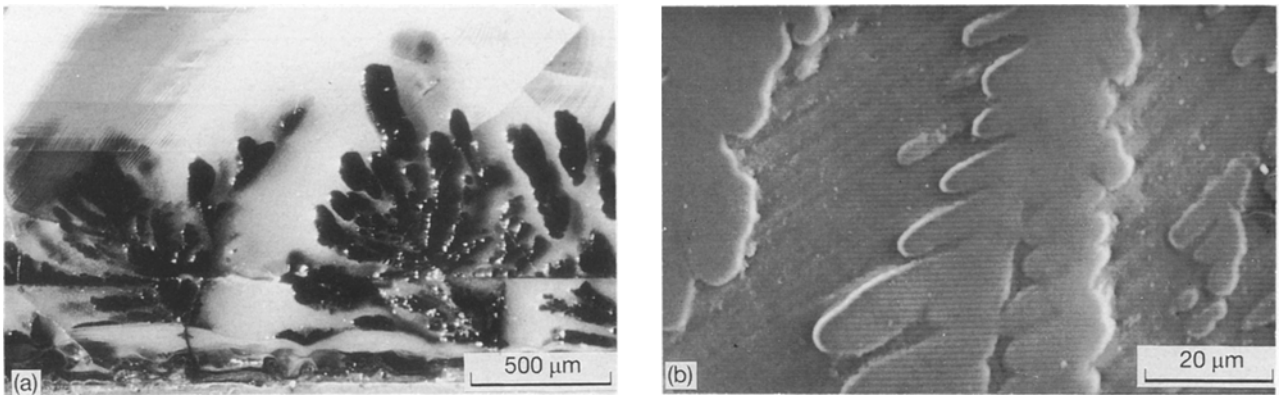

Figure 2 (a) Optical micrograph of a section of specimen RA6 showing inclusions of Mn-rich material in the sub-surface regions, and (b) scanning electron micrograph showing the migration of this material within the laminated weathering crust.

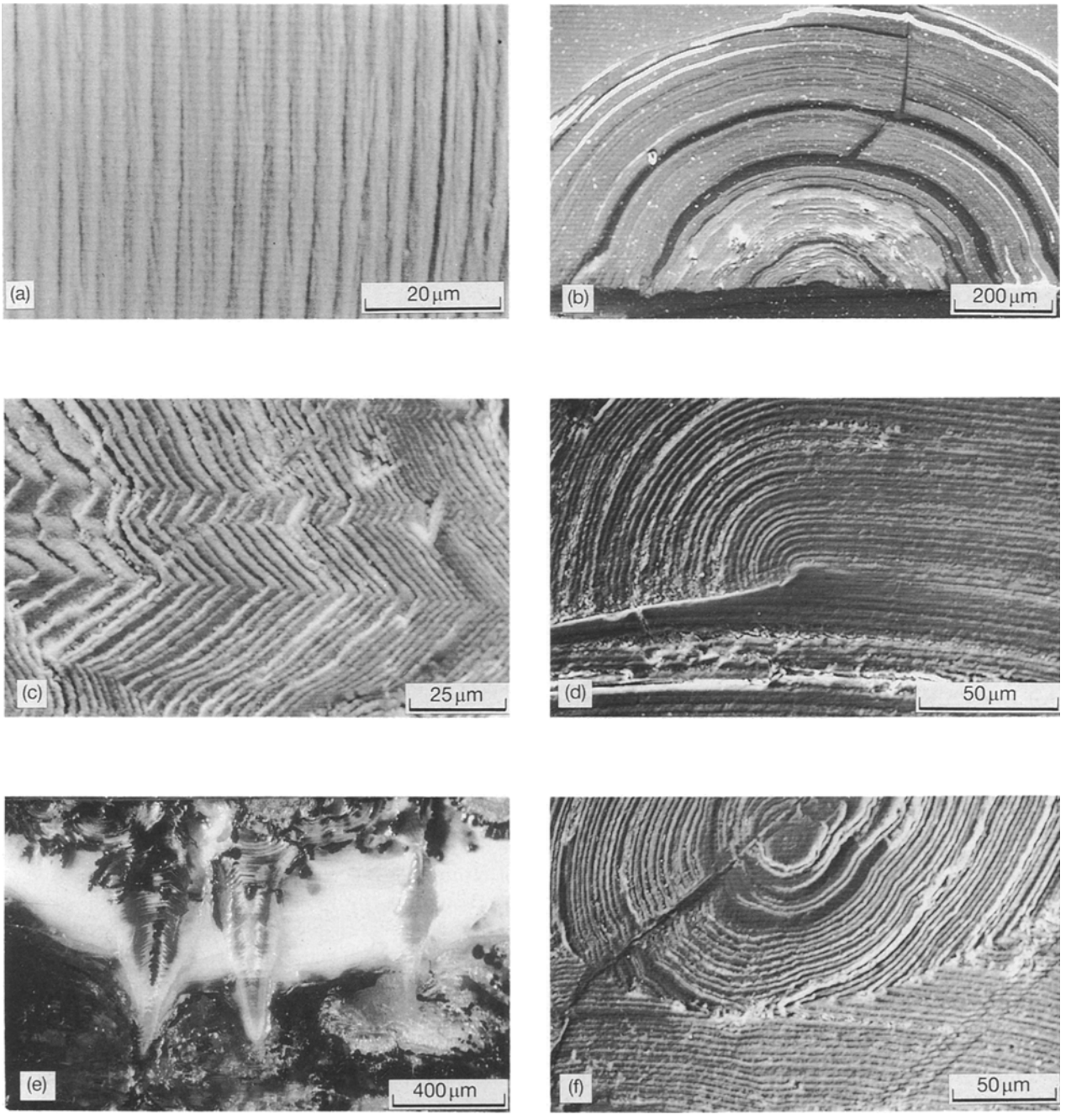

Figure 3 Scanning electron micrographs of sectioned, corroded glasses showing the morphology of the laminated weathering crusts: (a) parallel layers on specimen SC1; (b) hemispherical layers on specimen EP1; (c) zigzag banding on specimen EP1; (d) rotated bands on specimen EP1; (e) plugs of corrosion in specimen RA7; (f) complex system of layers caused by a gas bubble within specimen EP1.

distances varied: for potash glasses they were typically 2–15 μm; for soda glasses < 1 μm was more usual.

2. Hemispherical layers (Fig. 3b). When viewed in section, the advancing reaction zone was almost hemispherical, its centre located on the surface of the specimen. Such features rarely occurred in isolation. They had often developed independently from adjacent sites, then gradually coalesced as the corrosion fronts expanded into the unaltered glass. Remarkably, at the interface between two such systems, individual layers remained in correct register—see also Fig. 3f, where the same phenomenon occurs.

3. Zigzag banding (Fig. 3c). Bands of layers had developed a repeating, saw-tooth profile when seen in section. This type of morphology occurred where the corrosion had progressed in a direction parallel to linear inhomogeneities (cord and ream) present in the original glass. Zigzag banding was particularly prevalent in specimens from Eltham. Features of this type were observed by Raw [4]; they have recently been discussed by Cox and Ford [14].

4. Rotated bands (Fig. 3d). The regular progression of near-parallel layers has suffered a disturbance. This resulted in one region of the advancing corrosion front being rotated through an angle slightly > 90° to meet an existing band of layers whose development had previously been arrested.

5. Plugs (Fig. 3e). Intrusions, or plugs, of corrosion varied somewhat in profile. Commonly they were tapered and extended from the surface into the body of a specimen along a clearly-defined growth axis. The examples shown have developed independently of the main body of corrosion, as was revealed in the SEM. Surface microfissures, allowing groundwater to penetrate into the interior of the glass, were shown to be the origin of the plugs illustrated in Fig. 3e [15]. Salts in solution may precipitate along the core of plugs, as is clearly visible in the micrograph.

6. Complex morphologies (Fig. 3f). Arbitrarily complex systems of layers were present in most of the decayed glasses. Illustrated is an example of where a gas bubble, present in the pristine glass, had become connected, via a crack, to the advancing reaction zone. Layers of corrosion have expanded radially from the bubble, eventually meeting and coalescing with the planar corrosion front, which had independently progressed from the surface of the specimen. At the curved interface, individual layers remain in correct register.

The otherwise smooth progression of the corrosion may be locally disturbed by other types of inclusions, such as unmelted batch and foreign matter. However, in many cases the cause of complex morphological features could not be identified. Newton and Shaw [16] have illustrated such an example.

3.3. Concentration profiles of the weathering crusts

The chemical changes caused by prolonged aqueous attack of glass are further revealed by the concentration profiles of the constituents of the weathering crusts. Quantitative spot EPMA was carried out at regular intervals throughout the thickness of the corrosion on polished sections of potash glass. Data for specimen RA4 are shown in Fig. 4. They are representative, at least qualitatively, of the general behaviour of all such glasses examined in this manner.

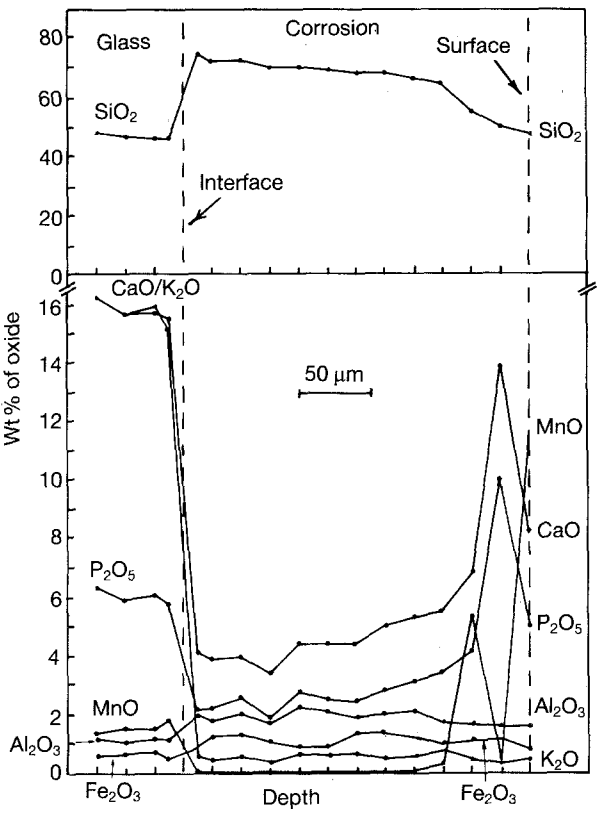

Figure 4 Concentration profiles of the principal constituents of the glass and weathering crust on specimen RA4.

At the glass–corrosion interface an enrichment of SiO_2 is evident, followed by a gradual decrease towards the surface. A silica-rich barrier was common to all specimens of weathered potash glass. In Table III the compositions of the unaltered glass and crust, measured near the interface, are compared for four sectioned specimens.

The K_2O, CaO and P_2O_5 concentrations in the corrosion show a sharp fall at the interface. This depletion was pronounced in the case of K_2O, which remained at a low level ($\lesssim$ 1 wt %) throughout the crust; MgO also behaved in this manner. For CaO and P_2O_5 the initial decrease was followed by a gradual recovery. A sharp fall then occurred in the near-surface region. The concentrations of Al_2O_3 showed an initial rise at the interface and thereafter continued at this elevated level.

The profiles of CaO and P_2O_5 were strongly correlated in the crusts, as shown in Fig. 4. A further point is that the MnO content rose steeply near the surface; this behaviour was noted in the crusts on all potash glasses, but was especially prominent in specimens from Rievaulx, for which surface concentrations reached values of almost 15 wt %. Both features suggest the diffusion of materials from the environment into the crusts, most probably in solution, followed by their deposition. These points are further discussed in section 3.4.2.

TABLE III Composition of glass compared with that of corrosion crust measured in close proximity to interface

Oxide	Wt % of oxide							
	EP1 Glass	Corrosion[a]	RA1 Glass	Corrosion[a]	SC6 Glass	Corrosion[a]	SAA1 Glass	Corrosion[b]
Na_2O	2.4	0.6	2.8	0.1	1.3	0.1	2.7	
MgO	7.3	0.3	6.2	0.2	7.0	0.6	6.5	
Al_2O_3	0.9	2.6	1.2	2.0	1.2	2.0	1.2	1.8
SiO_2	59.5	83.1	47.8	69.9	46.2	75.0	55.7	79.0
P_2O_5	3.0	1.7	5.9	2.0	6.9	6.3	3.1	1.1
K_2O	11.6	1.2	15.9	0.3	16.3	0.4	11.0	0.1
CaO	13.6	2.0	15.3	3.9	19.3	7.9	13.1	2.3
MnO	1.2	< 0.1	1.2		1.3	0.5	1.0	< 0.1
Fe_2O_3	0.8	1.2	0.9	1.4	0.6	1.2	0.6	1.0

Where no value is given that component was not detected.
[a] Measured at a distance of 10 μm from interface.
[b] Measured at a distance of 5 μm from interface.

TABLE IV XRD data for crystalline phases in the corrosion crust on specimen SC6

Sample number											
1		2		3		4		5		6	
d(nm)	*I*	d(nm)	*I*	d(nm)	*I*	d(nm)	*I*	d(nm)	*I*	d(nm)	*I*
0.302	10	0.305	70	0.303	70	0.305	100	0.303	100	0.303	100
0.274	100	0.273	100	0.273	100	0.274	90	0.272	90	0.268	60
0.235	50			0.234	40	0.234	40	0.236	20	0.232	10
								0.209	5	0.210	5
								0.192	5		
										0.188	5
0.163	10			0.157	10						
0.126	10	0.125	20	0.126	10						
		0.120	20								

Interplanar spacings (d) ± 0.002nm.
Relative intensities (I) are estimated.

As recorded in Table I the weathering layers on durable soda glasses from Wroxeter were < 40 μm in thickness, too thin to permit reliable concentration profiles of the constituents to be determined. However, qualitative X-ray line scans were obtained for the principal elements present in the layers. Results for specimen WRX6 are shown in Fig. 5.

A clear difference between the aqueous attack of soda–lime–silica glasses and their potash-containing counterparts is the absence of a silica-rich barrier at the glass–corrosion interface. Both Na and Ca are depleted in the thin crust on WRX6, whereas Al is enriched. No evidence was found for the surface enrichment of P, Ca or Mn in specimens from Wroxeter. This may be a consequence of the environment in which the glass had decayed, rather than a general feature of soda–lime–silica glass.

3.4. Crystalline phases within the crusts

3.4.1. The crust material

X-ray and electron diffraction studies revealed that the degree of crystallinity of the weathering crusts was either extremely low or undetectable. Specimens from Stamford produced the only recordable diffraction patterns. The *d*-values (interplaner spacings) for six powdered samples of crust material removed from specimen SC6 and subjected to XRD are given in Table IV. Extreme care was taken to exclude soil or extraneous matter.

The *d*-values were compared with published data for inorganic compounds in the "Powder Diffraction File Search Manual" (published by JCPDS, International Centre for Diffraction Data, Swarthmore, PA). No unique matches were established, but five crystalline phases possibly present are: $Na_2(Mn,Fe)_5(PO_4)_4$ (File no. 24–66); $Ca_2SiO_4H_2O$ (File no. 3–594); $Ca_3Mn_2Si_3O_{12}$ (File no. 27–85); Ca–Mg–Fe–Al–SiO_4–OH (File no. 30–253); and $Ca_3Al_2(SiO_4, CO_3,OH)_3$ (File no. 3–801).

Table IV shows that the relative intensities of the three most intense lines are not constant, suggesting the presence of several phases. Four of the compounds are calcium silicates or aluminosilicates; cationic replacement has occurred in three of them. These minerals are notoriously difficult to identify by means of XRD techniques when present at low concentrations.

3.4.2. Intruded materials

Intruded minerals were widely distributed throughout the crusts on potash glasses; there was no evidence for this on soda glasses. The most common were deposits of a hard, dark, lustrous material which occurred

predominantly in the near-surface regions, as shown in Fig. 2. It was especially prevalent in glasses from Eltham, Rievaulx and Stamford. Undoubtedly, this material had entered the decaying glass from the environment. In areas where the crusts were thin, optical microscopy revealed that its means of entry were scratches and other surface defects. When sectioned specimens were examined in the SEM, this mineral could be seen to have passed along fissures and then diffused—most probably in solution in groundwater—between the layers of corrosion, as may be seen in Fig. 2b. Analysis showed the main elements present to be Si, P, Ca, Mn and, to a lesser extent, Fe—see Table V.

An SEM micrograph of a sectioned region of crust on specimen RA3, which contains inclusions of this type, is illustrated in Fig. 6; X-ray elemental distribution maps ("dot maps") for the principal constituents are also shown. The close spatial correlation of Si and Al in the laminated crust is evident, whilst Ca, P and Mn are correlated in the areas where the intruded material has been precipitated. X-ray diffraction studies showed the latter to have a very low degree of crystallinity. The *d*-values for eight lines were determined, all of which closely matched those for calcite, $CaCO_3$.

On account of their number and size, the dark inclusions in specimen SC6 were subjected to laser Raman microspectroscopy. The spectrum showed a broad band with considerable structure centred at 960 cm^{-1}; subsidiary maxima occurred at 959, 961 and 965 cm^{-1}. A further maximum was located at 986 cm^{-1}. Reference spectra were obtained from high purity samples of several phosphates, including octacalcium phosphate, $Ca_8H_2(PO_4)_6 \cdot 5H_2O$; hydroxyapatite, $Ca_5(PO_4)_3OH$; and brushite, $CaHPO_4 \cdot 2H_2O$. The principal peaks in their Raman spectra occurred at 958, 960 and 986 cm^{-1}, respectively. This provides strong evidence in favour of these three modifications of calcium phosphate being present in the dark inclusions in the crusts on potash glasses. Other peaks in the spectrum could not be identified.

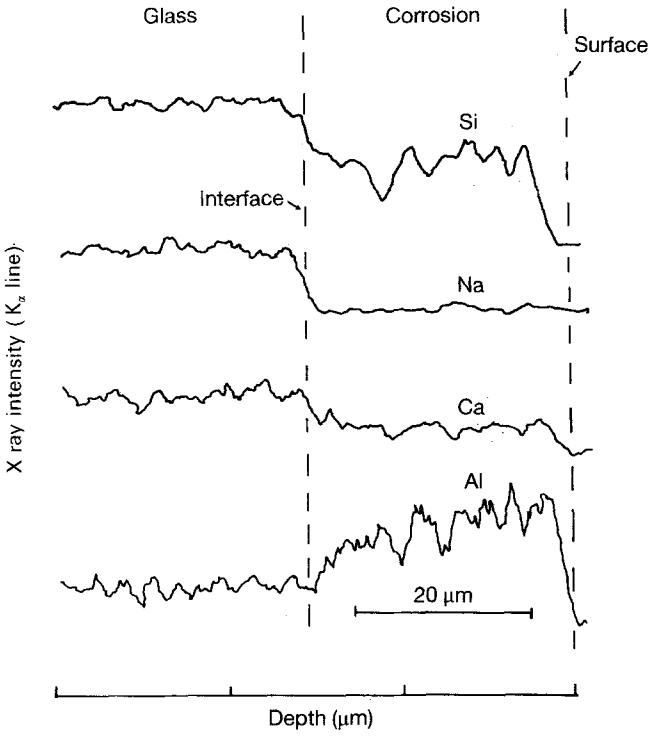

Figure 5 X-ray line scans for Si, Na, Ca and Al in the glass and weathering crust on specimen WRX6.

4. Thermodynamic stability of the glasses

Paul [17] predicted the durability of glass on the basis of its thermodynamic stability by assuming that glass–water interactions may be described in terms of the sum of the free energies of hydration (ΔG^0 values) of individual oxide or silicate groups, weighted in proportion to the mole fraction present. Newton and Paul [18] subsequently showed that ΔG^0 calculated in this manner correlated well with the amount of alkali leached from various glasses, the latter quantity being used as a measure of durability. Short-term laboratory tests on a variety of glasses, including ancient man-made and natural specimens, have demonstrated a linear relation between ΔG^0 and the release of structural silicon into the leaching solution [19].

In the present investigations, where aqueous attack of the glasses had already occurred, a measure of their relative durabilities could be determined only in terms of the mean rate of corrosion of the glasses, as revealed by the thickness of the weathering crusts which had formed during a known period of exposure to groundwater—see Table VI.

Mean rates of corrosion for specimens which retained their crusts intact were plotted against ΔG^0

TABLE V Mean composition of black intruded material

Specimen	Wt % of oxide								
	Na_2O	MgO	Al_2O_3	SiO_2	P_2O_5	K_2O	CaO	MnO	Fe_2O_3
EP1	0.4 ± 0.2	0.3 ± 0.1	1.9 ± 0.3	36.8 ± 2.0	2.8 ± 0.5	0.4 ± 0.2	5.9 ± 0.5	23.9 ± 2.0	2.0 ± 0.4
EP4	0.2 ± 0.1	0.2 ± 0.1	5.4 ± 0.4	46.5 ± 2.0	1.9 ± 0.3	3.5 ± 0.7	5.2 ± 0.5	10.8 ± 1.1	0.8 ± 0.3
RA6	0.4 ± 0.2	0.3 ± 0.1	1.6 ± 0.1	36.5 ± 5.0	10.8 ± 4.0	1.1 ± 0.5	17.6 ± 4.0	14.6 ± 4.4	0.8 ± 0.3
SC6	ND	ND	1.7 ± 0.2	28.0 ± 2.8	15.0 ± 1.8	ND	21.0 ± 3.0	9.3 ± 1.8	1.0 ± 0.2
SC10	ND	ND	1.7 ± 0.1	30.5 ± 8.0	19.5 ± 1.0	ND	27.7 ± 0.5	11.6 ± 2.0	0.8 ± 0.2
SC11	ND	ND	1.7 ± 0.1	29.5 ± 3.0	16.0 ± 5.0	ND	22.2 ± 6.0	9.8 ± 2.0	0.8 ± 0.2
SAA3	0.4 ± 0.2	0.2 ± 0.1	1.3 ± 0.2	30.2 ± 5.0	10.1 ± 4.0	0.8 ± 0.3	15.5 ± 5.0	15.2 ± 3.0	1.0 ± 0.2

ND Not determined.

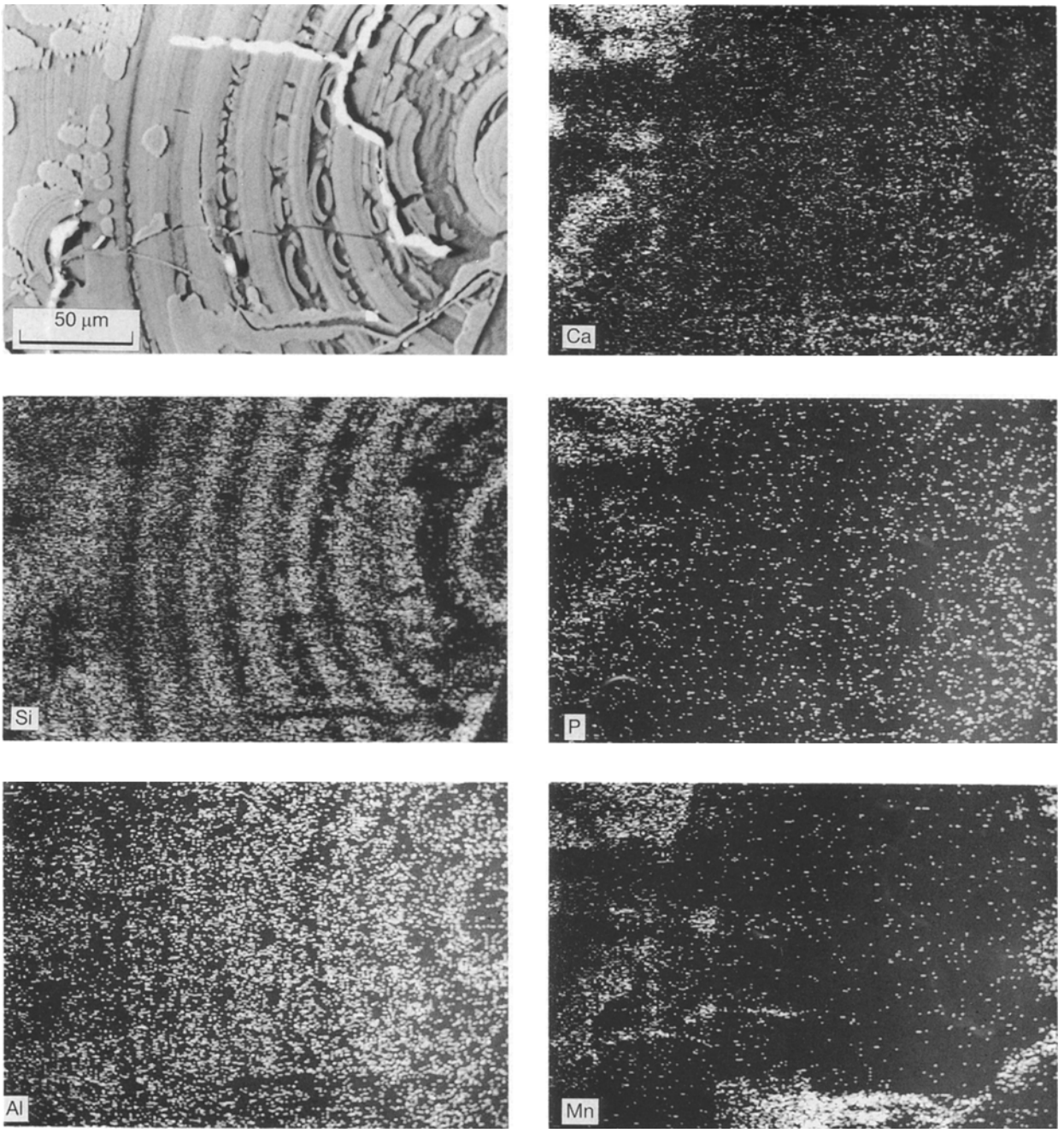

Figure 6 Scanning electron micrographs of specimen RA3 showing (top left) part of a system of hemispherical layers of corrosion with mineral inclusions (localized light areas) and elemental distribution maps for Si, Al, P, Ca and Mn. The layers are rich in Si and Al; the mineral inclusions are rich in Ca, P and Mn. The surface of the specimen is in the lower right hand corner of each micrograph.

values for the individual glasses. As shown in Fig. 7, a reasonably linear relationship exists between these two parameters. It should be noted that the more positive the free energy of hydration, the greater is the stability of the glass. Thus the poorly durable potash glasses (EP, RA, SAA and SC specimens) with ΔG^0 values in the range -25 to -40 kJ mol^{-1}, have the highest rates of corrosion amounting to slightly < 2 μm year^{-1}. Conversely, the stable soda glasses (WRX specimens) have ΔG^0 values of -15 to -17 kJ mol^{-1} and, in the most favourable cases, rates of surface layer formation $\leqslant 10^{-2}$ μm year^{-1}. Whether these rates were constant it is impossible to determine. The performance of the soda glasses is significantly better than the long-term ambient corrosion rate of 1 μm year^{-1}, calculated by Adams [20], for glasses of this type exposed to pure water.

5. Discussion

The reaction kinetics of the aqueous attack of silicate glasses have been widely investigated and quantified. Dissolution experiments, in which the surface of the leachate and the time-dependent composition of the leachant were analysed, have clarified the principal sequence of events.

Initially an ion-exchange process occurs in which alkali is released into solution and protons, most probably as H_3O^+ ions [21], and free water molecules [22, 23], enter the glass to produce a hydrated, alkali-deficient surface, or gel, layer [24, 25]. This first stage is diffusion controlled for pH values up to about 9 [26, 27].

A second stage, controlled by an interface reaction, reduces the thickness of the leached layer, thereby increasing the concentration gradient and regulating

TABLE VI Mean rates of corrosion and free energies of hydration

Specimen	Mean thickness of crust (μm)	Corrosion time (years)	Mean rate of corrosion (μm year^{-1})	Free energy of hydration $\Delta G°$(kJ mol^{-1})
EP1	657 ± 194	4.4×10^2	1.49	− 27.40
EP4	632 ± 83	4.4×10^2	1.44	− 29.22
RA1	ND	4.4×10^2		− 39.03
RA4	594 ± 93	4.4×10^2	1.35	− 39.91
RA6	764 ± 154	4.4×10^2	1.74	− 40.29
RA8	ND	4.4×10^2		− 40.55
SC6	1080 ± 130	7.7×10^2	1.40	− 42.19
SC10	ND	7.7×10^2		− 41.09
SC11	1000 ± 150	7.7×10^2	1.30	− 43.25
SAA1	320 ± 40	4.4×10^2	7.3×10^{-1}	− 27.55
SAA3	ND	4.4×10^2		− 38.54
WRX1	37	1.64×10^3	2.3×10^{-2}	− 15.81
WRX2	19	1.64×10^3	1.2×10^{-2}	− 15.36
WRX6	36	1.64×10^3	2.2×10^{-2}	− 12.78
WRX9	14	1.64×10^3	8.5×10^{-3}	− 16.97
WRX10	6	1.64×10^3	3.7×10^{-3}	− 15.19

ND patchy or highly irregular crust; mean thickness not determined.
All WRX glasses were very uniformly corroded.

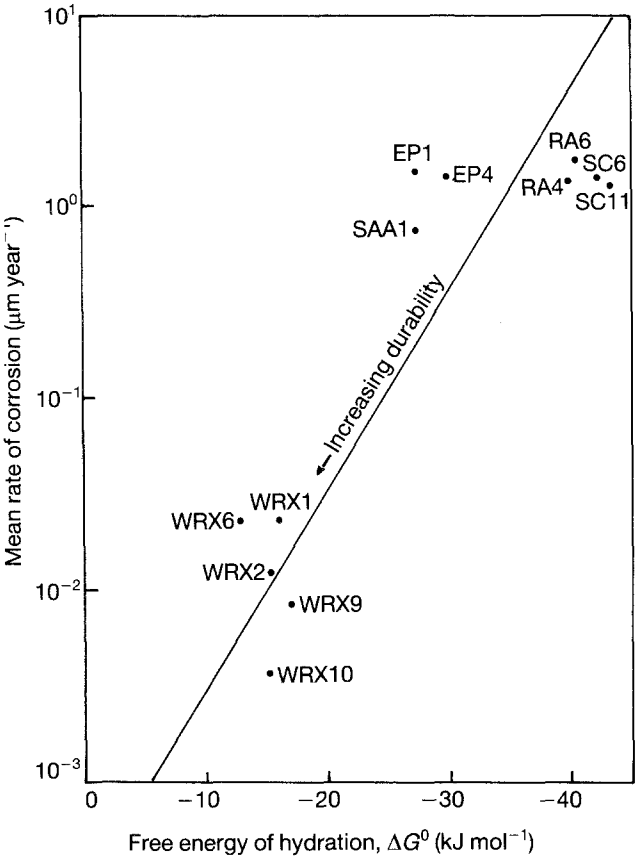

Figure 7 Mean rate of corrosion versus free energy of hydration of the pristine glasses.

the diffusion-controlled reaction [28]. Eventually the alkali-deficient layer attains a constant thickness; alkali, silica and other constituents are then extracted simultaneously (congruent dissolution). Above pH 9, the extraction of silica rapidly increases as a result of hydroxy ion (OH^-) attack of the silica bonds in the glass-forming network [24].

The subsequent precipitation of dissolution products on the surface of a specimen as secondary phases depends upon several factors, such as the extraction rate and solubility of the constituent oxides, especially silica and alumina, in the leachant. When solubility limits are exceeded precipitation occurs; this regulates the pH and concentration of the attacking solution at the reaction front. Thus cyclic reaction conditions prevail, resulting in the formation of layers of secondary alteration products [1]. The modelling of dissolution processes in HLW glasses and the release of radionuclides has been discussed by Grambow [29].

The variation in structure of the laminated crusts is remarkable; the cause, however, is rarely evident. Of the morphological types illustrated in Fig. 3, only two have been satisfactorily accounted for: zigzag banding and plugs. Inhomogeneities in the glass, inclusions such as gas bubbles, and surface defects have been shown to affect the progression of the reaction front. Surface stresses, caused for example by inadequate annealing of the finished product, could also be expected to exert an influence.

The formation of plugs of corrosion may have technological implications, since surface fissures in glass have been shown to be one means whereby they originate [15]. By facilitating the passage of water into the interior of a specimen, they promote its decay. The types of glass in which plugs occur have not been established, but should they develop in loaded HLW glasses, predictions of their long-term behaviour based upon leaching tests may be seriously in error. Similarly, the effects on durability produced by crustal deposits of hydroxyapatite, calcite or Mn-rich minerals is uncertain, but may be far reaching over millennia.

The compositional profiles and X-ray line scans shown in Figs 4 and 5 reveal the considerable extent to which the surface regions of the specimens have been chemically modified. Analytical data of this type have seldom been reported for man-made glasses that have undergone long-term dissolution by groundwater. Macquet and Thomassin [30] have recently published elemental profiles for five glasses (soda and potash) recovered from an archaeological site in France. The

fragments are of unspecified date, but would appear to have been buried for almost one thousand years. The leaching behaviour of both types of glass conforms closely with that reported here.

A further useful comparison is provided by the aqueous dissolution of natural glasses, such as tektites, basaltic and rhyolitic glasses over geological periods of time. Of relevance to the present study is that of Jercinovic *et al.* [31], who reported EPMA data for basaltic glasses (approximate composition in wt %: SiO_2 51, Al_2O_3 12, FeO 15, CaO 8, MgO 3.5, Na_2O 2.7, K_2O 1.5, P_2O_5 0.8, TiO_2 3.5) and their palagonites (hydration rinds). Following alteration by freshwater—as opposed to sea-water—the CaO, MgO, Na_2O and K_2O contents of the palagonites were always lower than in the corresponding glasses; the SiO_2, Al_2O_3 and FeO were depleted to lesser extents. These findings are in good agreement with the concentration profiles shown in Fig. 4.

The composition of groundwater is conditioned by the rock strata and soils through which it has percolated. In the present study Mn and Fe have entered the porous crusts in solution, initially through microcracks and other surface defects. Subsequently they have been precipitated, predominantly in the near-surface regions. Figs 2 and 6 illustrate this, whilst Table V provides relevant quantitative data. Geilmann [5] has published bulk analyses of crust material, where Mn and Fe concentrations are significantly enhanced relative to those in the glass—see Geilmann's Tables IV–VI.

Manganese and iron in the Mn(II) and Fe(II) states, respectively, are soluble in water but are thermodynamically unstable. They are readily oxidized to a higher, more stable, state to give insoluble compounds. Both elements are common constituents of soils as a result of the breakdown of silicate minerals. In natural waters, Mn concentrations as high as 10 p.p.m. have been recorded [32]. Thus, under anaerobic conditions, as in waterlogged soils, Mn(II) and Fe(II) ions are highly mobile, facilitating their migration in decomposing glass. However, should the oxygen content of the environment increase, due, for example, to the respiration of plants or biological activity, both elements may be precipitated as insoluble oxides. Marshall [33] lists bacteria, present in soils and aquatic environments, which are capable of transforming manganese to higher oxidation states. The complex chemical behaviour of Mn and Fe in soils has been discussed by Collins and Buol [34].

Fig. 6 shows that although the spatial distributions of Ca and P in the scanned area of corrosion are closely related, they are not coincident. As reported in section 3.4.2, the regions rich in Mn also contain deposits of hydroxyapatite and other modifications of calcium phosphate; calcite, too, occurs locally. That the composition of such regions is variable is reflected in the ratio CaO to P_2O_5, which varies within the range 1.2–1.5. Both constituents are present in significant amounts in the unaltered potash glasses (see Table II), but additional P (in the form of phosphate ions) and Ca appear to have entered into the crusts from the environment, as suggested by their high concentrations in the near-surface regions—see Fig. 4. The solubility of the various calcium phosphates decreases with increase in pH up to values of about 7.8 [35]. The pH of the soils from which the glasses were recovered was 7.2–7.9, as shown in Table I.

Crystalline alteration products have rarely been reported on man-made glass that has decayed naturally in soils at ambient temperatures. Freestone *et al.* [36] carried out XRD studies of surface crusts on excavated Near Eastern lead glasses dating to the 7th century BC; there was evidence to indicate the presence of lead hydroxyapatite, $Pb_5(PO_4)_3OH$, and pyromorphite, $Pb_5(PO_4)_3Cl$. The pristine glass had a low phosphorus content (< 0.20 wt % P_2O_5), suggesting that in this case, too, the phosphate had an external origin. Macquet and Thomassin [30] have reported hydrated calcium silicates; precise details of the compounds, or of the glasses on which they occurred, were not stated.

Various crystalline and amorphous phases have been identified on basaltic glasses that have undergone long-term palagonization in freshwater. They were mostly clays and zeolites whose composition depended upon the elements released from the glass and, in certain cases, upon the nature of the environment. Jercinovic *et al.* [31] found that of the clays iron-rich smectites were predominant. The zeolites analcime, $NaAlSi_2O_6 \cdot H_2O$, and thomsomite, $NaCa_2Al_5Si_5O_{20} \cdot 6H_2O$, were reported by Byers *et al.* [37] on synthetic basaltic glasses following hydrothermal leaching. The latter also detected calcite.

The secondary phases present on the surface of candidate HLW glasses subjected to hydrothermal dissolution are also chemically complex. The products formed at temperatures below 100 °C are largely amorphous hydrosilicates; regional crystallinity has, however, been observed [38]. At higher temperatures reformation of the compounds occurs, accompanied by recrystallization [39, 40]. Di- and tri-octahedral smectites, serpentines, zeolites and structurally simpler silicates, aluminosilicates and metal hydroxides have been identified [19, 41, 42].

With the exception of calcite, none of the phases identified in the surface layers on either natural or hydrothermally decomposed glasses was detected in the present study. The occurrence of calcite in porous materials that have remained in prolonged contact with groundwater is well known. Solutions which are saturated in calcium bicarbonate reprecipitate calcite according to changes in soil pH, water content and biological activity [43]. Whilst it is possible in the present study that part of the calcium content of this mineral may be derived from the glass, the carbonate must be entirely of external origin.

The identity of the phases which form on the surface of decomposing glass depends upon several factors, for example: the composition of the substrate; temperature; the nature and rate of replenishment of the leachant; pH; and other system variables [44]. When groundwater is the attacking medium, additional considerations arise, such as its complex geochemistry. The present study emphasizes this point. It also underlines the need for further research in this area if the

very long-term stability of glass in a natural environment is to be reliably predicted.

6. Conclusion

The surfaces of alkali–lime–silica glasses that had remained in prolonged contact with groundwater were severely modified, both physically and chemically. For soda and potash glasses the dominant dissolution process was the formation of multi-layered weathering crusts with complex morphologies and of a very low degree of crystallinity.

Relative to their substrates, the surface layers were almost totally depleted of Na_2O, K_2O and MgO; to lesser extents CaO and P_2O_5 were removed; Al_2O_3 and Fe_2O_3 generally remained at the same level or were slightly enriched. Although a SiO_2-rich barrier was present at the glass–corrosion boundary on potash glasses, it was insufficient to protect the glass from continuous aqueous attack. No such barrier was found in the case of soda glasses.

Values of the free energy of hydration of the specimens correlated well with the mean thickness of the weathering crusts. Soda glasses of high silica content (> 65 wt %) proved to be the most resistive to aqueous attack.

Within the crusts, localized deposits of minerals occurred. They were largely of external origin, indicating that the long-term behaviour of glass is not only a function of its composition, but is also strongly influenced by environmental factors, especially the geochemistry of the local groundwater.

Acknowledgements

We wish to thank the following for generously providing specimens of glass: Mrs M. E. Hutchinson and Dr C. A. Price of English Heritage, Historic Buildings and Monuments Commission for England, for specimens from Canterbury, Eltham and Rievaulx; Dr K. B. Pretty, New Hall, University of Cambridge, for specimens from Wroxeter; Ms S. Semmens and Ms C. M. Mahany, formerly of the Lincolnshire Trust for Archaeology, for specimens from Stamford. To the following members of staff of the University of York we express our gratitude: Dr I. Barkshire for assistance with the diffraction work; Professor R. E. Hester and Mr R. B. Girling for the use of, and assistance with, Raman microspectroscopy; the staff of the Soil Survey and Land Research Centre for determining the pH values of soil; and Mr S. Moehr for polishing the sectioned specimens. This research was carried out with the aid of SERC grant GR/D/63318, which we gratefully acknowledge.

References

1. W. LUTZE, in "Radioactive Waste Forms for the Future", edited by W. Lutze and R. C. Ewing (North-Holland, Amsterdam, 1988) p. 1.
2. W. L. BOURCIER, *Mater. Res. Soc. Symp. Proc.* **212** (1991) 3.
3. D. BREWSTER, *Phil. Trans. R. Soc. Edinb.* **23** (1863) 193.
4. F. RAW, *J. Soc. Glass. Technol.* **39** (1955) 128T.
5. W. GEILMANN, *Glastech. Ber.* **29** (1956) 145.
6. R. H. BRILL and H. P. HOOD, *Nature* **189** (1961) 12.
7. R. G. NEWTON, *Archaeometry* **13** (1971) 1.
8. G. MALOW, *Mater. Res. Soc. Symp. Proc.* **11** (1982) 25.
9. G. A. COX and B. A. FORD, *J. Mater. Sci.* **24** (1989) 3146.
10. G. C. COPPACK, private communication.
11. G. LOVE, in "Quantitative Electron-Probe Microanalysis", edited by V. D. Scott and G. Love (Ellis Horwood, Chichester, 1983) p. 234.
12. E. R. CALEY, in "Analyses of Ancient Glasses 1790–1957" (Corning Museum of Glass, New York, 1962) p. 93.
13. K. J. S. GILLIES and A. COX, *Glastch. Ber.* **61** (1988) 75.
14. G. A. COX and B. A. FORD, *Glass Technol.* **30** (1989) 113.
15. G. A. COX and A.-R. KHOOLI, *ibid.* **33** (1992) 60.
16. R. G. NEWTON and G. SHAW, *ibid.* **29** (1988) 78.
17. A. PAUL, *J. Mater. Sci.* **12** (1977) 2246.
18. R. G. NEWTON and A. PAUL, *Glass Technol.* **21** (1980) 307.
19. C. M. JANTZEN and M. J. PLODINEC, *J. Non-Cryst. Solids* **67** (1984) 207.
20. P. B. ADAMS, *ibid.* **67** (1984) 193.
21. R. H. DOREMUS, *ibid.* **19** (1975) 137.
22. F. M. ERNSBERGER, *Phys. Chem. Glasses* **21** (1980) 146.
23. H. SCHOLZE, *Glastech. Ber.* **58** (1985) 116.
24. R. W. DOUGLAS and T. M. EL-SHAMY, *J. Amer. Ceram. Soc.* **50** (1967) 1.
25. T. M. EL-SHAMY and R.W. DOUGLAS, *Glass Technol.* **13** (1972) 77.
26. C. R. DAS, *J. Amer. Ceram. Soc.* **63** (1980) 160.
27. J. C. DRAN, J. C. PETIT, T. TROTIGNON, A. PACCAGNELLA and G. DELLA MEA, *Mater. Res. Soc. Symp. Proc.* **127** (1989) 25.
28. W. A. LANFORD, K. DAVIS, P. LAMARCHE, T. LAURSEN and G. GROLEAU, *J. Non-Cryst. Solids* **33** (1979) 249.
29. B. GRAMBOW, in "Safety Assessment of Radioactive Waste Repositories, Proceedings of the Symposium, Paris, 1989", (Organisation for Economic Cooperation and Development, Paris, 1990) p. 439.
30. C. MACQUET and J. H. THOMASSIN, *Appl. Clay Sci.* 7 (1992) 17.
31. M. J. JERCINOVIC, R. C. EWING and C. D. BYERS, in "Advances in Ceramics, Vol. 20, Nuclear Waste Management II, Chicago 1986", edited by D. E. Clark, W. B. White and A. J. Machiels (American Ceramic Society, Westerville, OH) p. 671.
32. J. J. MORGAN and W. STUMM, *J. Amer. Water Works Assoc.* **57** (1965) 107.
33. K. C. MARSHALL, in "Biochemical Cycling of Mineral-Forming Elements" edited by P. A. Trudinger and D. J. Swaine (Elsevier Scientific Publishing, Amsterdam, 1979) p. 261.
34. J. F. COLLINS and S. W. BUOL, *Soil Sci.* **110** (1970) 111.
35. W. L. LINDSAY, in "Chemical Equilibria in Soils" (Wiley Interscience, New York, 1979) Fig. 12.8.
36. I. C. FREESTONE, N. D. MEEKS and A. P. MIDDLETON, *Archaeometry* **27** (1985) 161.
37. C. D. BYERS, R. C. EWING and M. J. JERCINOVIC in "Advances in Ceramics, Vol. 20, Nuclear Waste Management II, Chicago, 1986", edited by D. E. Clark, W. B. White and A. J. Machiels (American Ceramic Society, Westerville, OH) p. 733.
38. J. F. FLINTOFF and A. B. HARKER, *Mater. Res. Soc. Symp. Proc.* **44** (1985) 147.
39. G. J. McCARTHY, B. E. SCHEETZ, S. KOMARNENI, D. K. SMITH and W.B. WHITE. in "Solid State Chemistry: A Contemporary Overview", edited by S. L. Holt, J. B. Milstein and M. Robbins (American Chemical Society Advances in Chemistry Series, 186, 1980) p. 349.
40. D. SAVAGE, J. E. ROBBINS and R. J. MERRIMAN, *Mineral. Mag.* **49** (1985) 195.
41. J. K. BATES, L. J. JARDINE and M. J. STEINDLER, *Science* **218** (1982) 51.
42. W. LUTZE, in "Radioactive Waste Forms for the Future", edited by W. Lutze and R. C. Ewing (North-Holland, Amsterdam, 1988) 128.
43. M. A. COURTY, P. GOLDBERG and R. MACPHAIL, in "Soils and Micromorphology in Archaeology" (Cambridge University Press, Cambridge, 1989) p. 172.
44. B. GRAMBOW, in "Advances in Ceramics", Vol. 8, edited by G. G. Wicks and W. A. Ross (American Ceramic Society, Columbus, OH, 1984) p. 474.

Received 24 September
and accepted 8 December 1992